Activation and Inactivation of Homomeric KvLQT1 Potassium Channels

Michael Pusch,* Raffaella Magrassi,* Bernd Wollnik,# and Franco Conti*
*Istituto di Cibernetica e Biofisica, CNR, I-16149 Genoa, Italy, and #Child Health Institute, Department of Medical Genetics, Istanbul University, 34290 Istanbul, Turkey

ABSTRACT The voltage-gated potassium channel protein KvLQT1 (Wang et al., 1996. *Nature Genet.* 12:17–23) is believed to underlie the delayed rectifier potassium current of cardiac muscle together with the small membrane protein minK (also named IsK) as an essential auxiliary subunit (Barhanin et al., 1996. *Nature.* 384:78–80; Sanguinetti et al., 1996. *Nature.* 384:80–83). Using the *Xenopus* oocyte expression system, we analyzed in detail the gating characteristics of homomeric KvLQT1 channels and of heteromeric KvLQT1/minK channels using two-electrode voltage-clamp recordings. Activation of homomeric KvLQT1 at positive voltages is accompanied by an inactivation process that is revealed by a transient increase in conductance after membrane repolarization to negative values. We studied the recovery from inactivation and the deactivation of the channels during tail repolarizations at −120 mV after conditioning pulses of variable amplitude and duration. Most measurements were made in high extracellular potassium to increase the size of inward tail currents. However, experiments in normal low-potassium solutions showed that, in contrast to classical C-type inactivation, the inactivation of KvLQT1 is independent of extracellular potassium. At +40 mV inactivation develops with a delay of 100 ms. At the same potential, the activation estimated from the amplitude of the late exponential decay of the tail currents follows a less sigmoidal time course, with a late time constant of 300 ms. Inactivation of KvLQT1 is not complete, even at the most positive voltages. The delayed, voltage-dependent onset and the incompleteness of inactivation suggest a sequential gating scheme containing at least two open states and ending with an inactivating step that is voltage independent. In coexpression experiments of KvLQT1 with minK, inactivation seems to be largely absent, although biphasic tails are also observed that could be related to similar phenomena.

INTRODUCTION

Cardiac delayed rectifier potassium currents are important for the repolarization of the cardiac action potential (Noble, 1984; DiFrancesco, 1985; Campbell et al., 1992; Roden and George, 1996). At least two types of potassium currents are believed to contribute to the repolarization of the cardiac action potential (Balser et al., 1990; Jurkiewicz and Sanguinetti, 1993). A rapid pseudo-inwardly rectifying current, I_{Kr}, and a much slower current, I_{Ks}. It is now believed that I_{Kr} is mediated by the gene product of the human ether-a-gogo-related gene (HERG) (Sanguinetti et al., 1995; Trudeau et al., 1995), and that I_{Ks} is due to a heteromeric association of the *KVLQT1* gene product with the minK protein (Barhanin et al., 1996; Sanguinetti et al., 1996). The contribution of HERG and KvLQT1 to cardiac potassium channels is strongly supported by their involvement in the inherited long QT syndrome, characterized by cardiac arrhythmia (Curran et al., 1995; Wang et al., 1996a).

Whereas the HERG channel reproduces most of the properties of the pseudo-inwardly rectifying cardiac K^+ current when it is heterologously expressed, e.g., in *Xenopus* oocytes (Smith et al., 1996; Wang et al., 1996b; Spector et al., 1996), this is not true for the KvLQT1 protein. When KvLQT1 is expressed alone in *Xenopus* oocytes or mammalian cells, rapidly activating K^+ currents are observed (Barhanin et al., 1996; Sanguinetti et al., 1996). Only the coexpression of KvLQT1 with minK leads to slowly activating K^+ currents with characteristics similar to those of the native cardiac I_{Ks} current (Barhanin et al., 1996; Sanguinetti et al., 1996; Yang et al., 1997). Furthermore, the small minK protein (Takumi et al., 1988) alone induces a slowly activating K^+ current when expressed in *Xenopus* oocytes (Takumi et al., 1988; see Kaczmarek and Blumenthal, 1997 for review), but it has long been a matter of debate whether minK forms an ion channel on its own (Kaczmarek and Blumenthal, 1997). It is now believed that the currents observed after minK expression are due to a heteromerization with an endogenous *Xenopus* KvLQT1 homolog (Sanguinetti et al., 1996). Evidence has also been reported for an association of minK with HERG, even though, apart from increasing the absolute current amplitude, functional properties were changed only slightly (McDonald et al., 1997).

To understand how the association with the minK subunit leads to such a profound alteration in channel gating, we sought to investigate in detail the gating of KvLQT1 alone and in coexpression with minK. Using tail-pulse protocols a rather complex gating of KvLQT1 is revealed. In particular, we find that the activation of homomeric KvLQT1 is accompanied by a delayed inactivation and that the rapid saturation of outward currents arises from the balance between slower contrasting processes of opening and inactivation of channels.

In coexpressions with minK, the inactivation process seems to be largely absent. We conclude that one effect of

Received for publication 14 November 1997 and in final form 29 April 1998.

Address reprint requests to Dr. Michael Pusch, Istituto di Cibernetica e Biofisica, CNR, Via de Marini 6, I-16149 Genova, Italy. Tel.: +39-10-6475-561; Fax: +39-10-6475-500; E-mail: pusch@barolo.icb.ge.cnr.it.

0006-3495/98/08/785/08 $2.00

the association with minK is to mask or to suppress the inactivation mechanism present in homomeric KvLQT1 channels by slowing or preventing the transition to an open state from which inactivation occurs.

MATERIALS AND METHODS

cRNA synthesis and oocyte injection

Capped RNA was transcribed by SP6 RNA polymerase from the isoform 0 of KvLQT1 (Wollnik et al., 1997) and of the minK protein (Takumi et al., 1988; Wollnik et al., 1997) after linearization with *Mlu*I or *Sna*BI, using the mMessage mMachine cRNA synthesis kit (Ambion) according to the instructions of the manufacturer. About 10 ng KvLQT1 cRNA (for homomeric KvLQT1 channels) or 5 ng KvLQT1 cRNA + 0.5 ng minK cRNA (for heteromeric channels) was injected per oocyte.

Xenopus laevis ovaries were obtained from frogs that had been anaesthetized with tricaine (0.17%) for 15–30 min. After surgery suitable aftercare was given. Ovaries were treated for 90 min with collagenase (1 mg/ml Sigma type II) in a solution containing 88 mM NaCl, 2.4 mM $NaHCO_3$, 1.0 mM KCl, 0.33 mM $CaNO_3$, 0.82 mM $MgSO_4$, 10 mM Tris Cl, pH 7.6, to remove the follicular layer.

Oocytes were kept in Barth's solution (88 mM NaCl, 2.4 mM $NaHCO_3$, 1.0 mM KCl, 0.41 mM $CaCl_2$, 0.33 mM $CaNO_3$, 0.82 mM $MgSO_4$, 10 mM Tris-Cl, pH 7.6).

Recording solutions

Initially, the following solutions were used as extracellular bath solutions (amounts are in mol/liter; Hepes was titrated with NaOH; pH 7.4 for all solutions):

100 Na: 100 NaCl, 0.5 $CaCl_2$, 3 $MgCl_2$, 5 HEPES

100 K: 100 KCl, 0.5 $CaCl_2$, 3 $MgCl_2$, 5 HEPES

In the experiments shown in Fig. 2, KCl was replaced with K-gluconate. This did not change the current characteristics.

Electrophysiology and data analysis

Standard two-electrode voltage-clamp measurements were performed 2–5 days after injection at room temperature (22–24°C), using a home-made high-voltage amplifier, a 12-bit AD/DA interface (Instrutech Corp., Mineola, NY) attached to an Atari Mega 4 computer, and the Patch data acquisition program (version 2.02; Instrutech Corp.). Data were analyzed using home-written software (written in Visual C++; Microsoft) and the SigmaPlot program (Jandel Scientific, Corte Madeira, CA). All fitting procedures were based on a least-squares criterion and the simplex algorithm (Caceci and Cacheris, 1984).

Voltage-clamp protocols are described in the figure legends. The holding potential in all recordings was −80 mV, except for the one shown in Fig. 6 *c*.

Leakage currents were subtracted using steps in the range from −120 mV to −80 mV, assuming that all channels are closed at voltages ≤ −80 mV for Figs. 1, 2, 5, and 6, *a* and *b*. In some figures the capacitive transients were blanked for reasons of clarity.

RESULTS

Expression of KvLQT1 gives rise to outwardly rectifying potassium currents in *Xenopus* oocytes (Barhanin et al., 1996; Sanguinetti et al., 1996; Yang et al., 1997), as shown in Fig. 1 *a*. Recording a similar *I-V* relationship in high extracellular potassium reveals a large inward potassium current on return to −80 mV, which subsides slowly with a time constant of 300 ms, but increases at early times as if the fastest process induced by the repolarization were the recovery from an inactivation process (Fig. 1 *b*). Such a "hook" in the tail currents has been described briefly in earlier reports (Sanguinetti et al., 1996; Yang et al., 1997) and in abstract form (Tristani-Firouzi et al., 1997). As seen in Fig. 1 *a*, a similar biphasicity is also present in a high Na^+ solution, where the tail currents are in the outward direction, supporting the idea that it is a distinguishing feature of the potassium selective conductance induced by expression of KvLQT1 channels. No such feature was ever observed in noninjected oocytes.

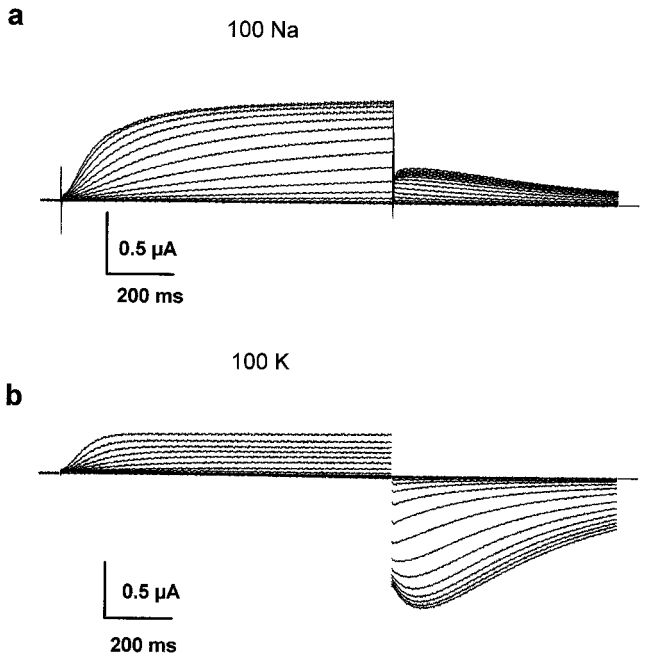

FIGURE 1 Families of voltage-clamp traces of homomeric KvLQT1 channels in 100 Na (*a*) and 100 K (*b*) solution. From a holding potential of −80 mV, the voltage was stepped to values up to +60 mV in 10-mV increments. Linear leak subtraction was performed using the responses to steps from −80 to −120 mV.

We sought to investigate the above phenomenon in more detail, to resolve the activation and inactivation properties of KvLQT1 channels. Most of the recordings were performed in high extracellular K^+ to improve the signal-to-noise ratio, because the gating characteristics seem to exhibit only a slight dependence on the external K^+ concentration (see Fig. 5).

Envelopes of tail currents at a tail potential $V_t = -120$ mV, after prepulses of increasing duration, t_p, at any voltage, V_p, were used to study the development of activation and inactivation processes during the step to V_p. Fig. 2 shows the pulse protocol (Fig. 2 *a*) and a series of recordings for t_p increasing from 100 ms to 1.5 s in steps of 100 ms and for $V_p = -40$ mV (Fig. 2 *b*), $V_p = 10$ mV (Fig. 2 *c*), and $V_p = +50$ mV (Fig. 2 *d*). The most striking feature of the gating characteristics of KvLQT1 at positive V_p is that even though the prepulse current and the "instanta-

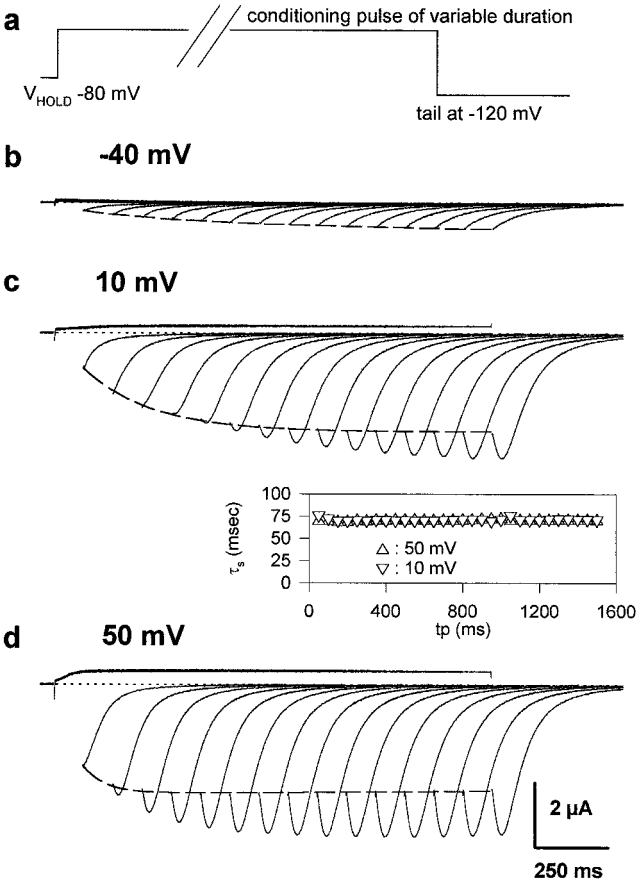

FIGURE 2 Envelope of tail currents at various conditioning voltages. (*a*) The voltage-clamp protocol. (*b–c*) The voltage-clamp traces with variable conditioning pulse durations are shown superimposed for each of the indicated voltages. Linear leakage was subtracted as in Fig. 1. The dashed lines are drawn by eye and connect the instantaneous tail currents. Note the slight decrease in these instantaneous currents for the conditioning voltage of +50 mV. The inset shows the t_p dependence of τ_s at +50 and +10 mV.

neous" tail current reach a plateau after short times, the shape of the tail current keeps changing at larger t_p, demonstrating that the channels are still undergoing a slower gating process. Indeed, the tail "hook," indicative of recovery from an inactivation process, also appears with a considerable delay. For example, the series of records of Fig. 2 *d* shows no appreciable tail current biphasicity for $t_p = 100$ ms, although the instantaneous tail current has already reached 75% of its maximum value. We notice from the same series that some ongoing inactivation process is also suggested by a slight late decay of the envelope of the initial tail currents. However, inactivation is much more apparent in the tail relaxations at −120 mV that reveal a deinactivation process faster than closing.

For a quantitative characterization, the currents recorded during any time segment at the voltage V were first converted to conductance G by dividing by $(V - V_{rev})$, where V_{rev} is the reversal potential of the KvLQT1 currents (≈ -10 mV in high K solutions). The biphasic time course of the tail conductance was then fitted with a double-exponential function of the form

$$G(t) = a_s \exp(-t/\tau_s) - a_f \exp(-t/\tau_f) \quad (1)$$

with a fast time constant τ_f and a slow time constant τ_s. When the tail was well fitted by a single exponential (for short prepulses and/or for small prepulse depolarisations), its amplitude and time constant were taken as a_s and τ_s, whereas a_f was set to zero. An example of a double-exponential fit of tail conductance for one of the records of Fig. 2 *d* ($V_p = 50$ mV, $t_p = 1000$ ms) is shown in Fig. 3. The fast negative component with an amplitude $a_f = 71$ µS and a time constant $\tau_f = 27$ ms is responsible for the initial rise, whereas the late decay is dominated by the slow component with an amplitude $a_s = 98$ µS and a time constant $\tau_s = 75$ ms. A key feature of the tail relaxations at −120 mV, fairly appreciable from Fig. 2, is that neither τ_s nor τ_f (when measurable) shows significant dependence on the voltage and duration of the conditioning prepulse (see *inset* in Fig. 2 for τ_s). Experiments on seven different oocytes yielded $\tau_f = 28 \pm 4$ ms and $\tau_s = 73 \pm 5$ ms (mean ± SD). The independence of the kinetics of tail relaxations from V_p and t_p was true also for tail potentials between −110 and −60 mV. Measurements of tail currents at these potentials after a prepulse to +40 mV ($n = 6$; see, e.g., Fig. 5) were well fitted by a double-exponential function with time constants that did not vary significantly for t_p between 0.4 and 2 s. Likewise, the tail relaxations for *I-V* protocols as in Fig. 1 also confirmed at $V_t = -80$ mV the independence of τ_s and τ_f from the prepulse voltage ($n = 4$). This independence is compatible with a deactivation process of KvLQT1 channels at negative voltages that can be described by a kinetic scheme containing only three states, indicating that the closing transitions are mainly fed (directly or indirectly) by the rate-limiting exit from only two states: an open state and an inactivated state. According to this view, a "hook" in the tail conductance implies that the channels that close after a negative step repolarization are less than those that open from the inactivated state. More generally, also when no real "hook" is observed, we assume tentatively that for $V_t =$

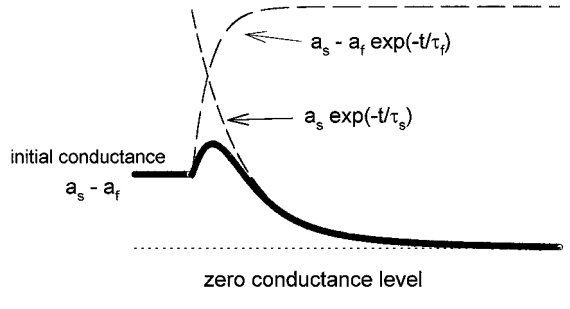

FIGURE 3 Biphasic, double-exponential time course of the tail conductance at −120 mV. A voltage-clamp trace at a conditioning voltage of +50 mV (duration 1000 ms) was converted to conductance by scaling with the driving force of −110 mV (*heavy solid curve*) and is shown superimposed with a double exponential fit (Eq. 1) (*solid line, not visible below the heavy solid curve*). The two exponential components of the fit are shown as dashed lines.

−120 mV, the amplitude a_f is related to the degree of inactivation, whereas a_s indicates roughly the degree of activation (thought as total probability of open or reopenable inactivated states) at the end of the conditioning pulse, even though this assignment is at most very qualitative (see Discussion).

The time (t_p) and voltage (V_p) dependence of a_s and a_f is shown in Fig. 4. The data are averages from seven experiments of the type illustrated in Figs. 2 and 3. For a more meaningful averaging, the values of a_s and a_f were normalized to the largest measured a_s value (for $V_p = +50$ mV and $t_p = 1.5$ s) that ranged in the different experiments from 30 to 120 μS. In Fig. 4, different symbols are used to plot the time course of a_s and a_f at different voltages (from −60 to +50 mV). It is seen that the development of both components is initially sigmoidal (more so in the case of a_f), but is well fitted after a certain time by single exponentials shown in the figure as continuous curves. The late time constant for the development of a_s at +40 mV is ~300 ms.

A similar inactivation process that kinetically overlaps with activation was observed in the pseudo-inwardly rectifying HERG K^+ channel (Smith et al., 1996; Wang et al., 1996b; Spector et al., 1996; Schönherr and Heinemann, 1996). In that case the mechanism was assumed to have several characteristics of the so-called C-type inactivation of Shaker K^+ channels, which has the hallmark of being strongly dependent on extracellular K^+ concentration, $[K]_o$ (Hoshi et al., 1990; López-Barneo et al., 1993; Baukrowitz and Yellen, 1995). We asked if the inactivation of KvLQT1 has a similar $[K]_o$ dependence. Fig. 5 shows the comparison of tail current measurements from the same oocyte in a low-K^+ or a high-K^+ solution. Fig. 5, *a* and *b*, shows recordings in the two conditions with the same pulse protocol ($V_p = +40$ mV, V_t varying from −110 to −40 mV in steps of 10 mV). In both cases, a biphasic time course of the

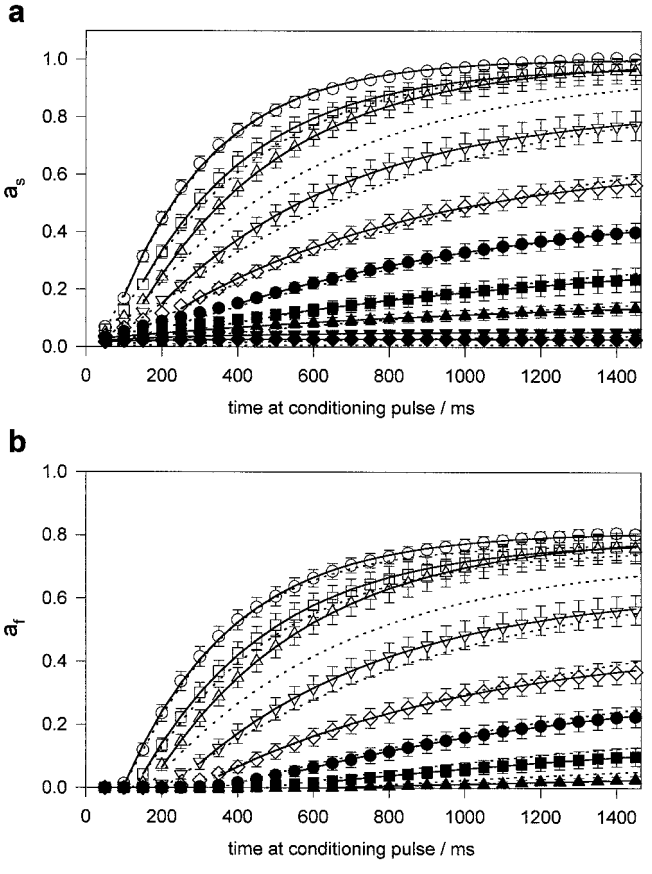

FIGURE 4 Fast and slow component of a double-exponential fit to the tail currents from experiments as shown in Fig. 2. The slow component, a_s (*a*), and the fast component, a_f (*b*), are shown as a function of the duration of the conditioning pulse at various prepulse voltages (○, 50 mV; □, 40 mV; △, 30 mV; ▽, 20 mV; ◇, 10 mV; ●, 0 mV; ■, −10 mV; ▲, −20 mV; ▼, −40 mV; ◆, −60 mV). The values were normalized to the maximum value obtained for a_s at +50 mV after a prepulse to 1.5 s, and the average from measurements from seven different oocytes was calculated (error bars indicate SEM). Solid lines represent fits with single exponential functions only for the late phase. Dotted lines represent predictions of Scheme 2 with two closed states and the parameters given in the legend of Fig. 8.

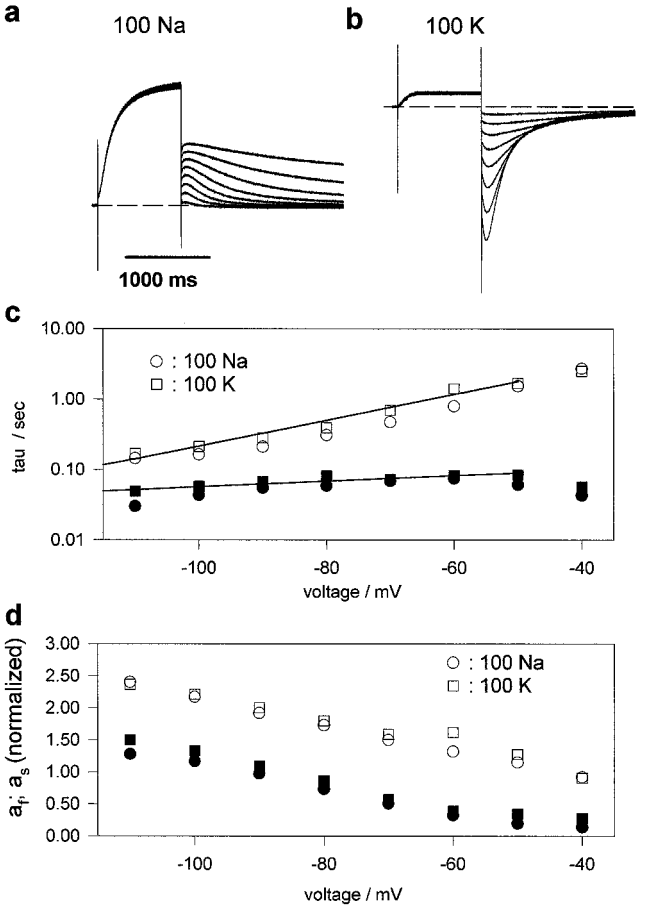

FIGURE 5 Independence of tail current kinetics on the extracellular K^+ concentration. Tail currents were elicited after a fixed prepulse to +40 mV to various tail potentials in 100 Na (*a*) and 100 K (*b*). Double-exponential fits (Eq. 1) to the tail currents yielded fast (*filled symbols*) and slow (*open symbols*) time constants as shown in *c*. The solid lines in *c* are fits of Eq. 3 to the time constants in 100 K for $V < -40$ mV, with $z = 1$ for the slow time constant and $z = 0.2$ for the fast time constant. The amplitudes a_f (*filled symbols*) and a_s (*open symbols*) after normalization to the instantaneous tail current are shown in *d*.

tail current can be seen at all tail voltages, and a good fit was obtained with a double-exponential function. The least-squares fitted time constants and amplitudes are shown in Fig. 5, *c* and 5 *d*, respectively. The values for $[K]_o = 0$ or 100 mM are very similar, showing that in this respect the inactivation of KvLQT1 is quite distinct from Shaker C-type inactivation.

No indication of an inactivation process as extensive as the one described above is seen in recordings of the currents mediated by heteromeric KvLQT1/minK channels, which are activated by much longer pulse durations with activation kinetics ~10-fold slower than homomeric KvLQT1 channels. Fig. 6 *a* shows that a depolarization of 8 s at +40 mV, causing almost full activation of these channels, is followed by almost monoexponential tail currents at the time resolution used in these recordings (*dashed lines* in Fig. 6 *a* represent monoexponential fits to the tail currents for $V_t < -20$ mV). The time constants range between 800 ms at −80 mV and 1.3 s at −40 mV, being comparable to those of the slow component of the deactivation of homomeric KvLQT1 (see Fig. 5 *c*). A monophasic time course is also observed on an expanded time scale for a much shorter prepulse duration (Fig. 6 *b*). A slightly biphasic deactivation becomes apparent only after the membrane potential is held at +40 mV for more than 20 s, in which case an inflection of the tail currents at negative potentials reveals the presence of a relatively fast relaxation that partially counteracts deactivation (Fig. 6 *c*).

In contrast to the gating characteristics, the instantaneous current-voltage relationship of KvLQT1 is not altered by association with minK, as shown in Fig. 7. Like heteromeric KvLQT1/minK channels, homomeric KvLQT1 channels are slightly inwardly rectifying in almost symmetrical solutions.

DISCUSSION

In this paper we have analyzed a peculiarity of the gating of homomeric KvLQT1 channels that is absent or strongly attenuated in KvLQT1/minK heteromers. Understanding how the association with minK modifies the gating characteristics of KvLQT1 is important to gaining insights into the functioning of this cardiac delayed rectifier K^+ channel. Heteromeric KvLQT1/minK channels reproduce the slow kinetics of the cardiac delayed rectifier potassium current, whereas the homomeric assembly of KvLQT1 subunits mediates a relatively fast outward rectifying current (Barhanin et al., 1996; Sanguinetti et al., 1996; Yang et al., 1997). We show here that the peculiar "hook" of the tail currents of homomeric KvLQT1 channels briefly described in earlier reports (Sanguinetti et al., 1996; Yang et al., 1997; Tristani-Firouzi et al., 1997) reveals a distinctive feature of the gating of these channels: a delayed inactivation that is hardly appreciable as a late decline in the currents activated at positive voltages, but shows up as a biphasic deactivation during negative repolarizations.

Is this inactivation mechanistically equivalent to the inactivation of HERG channels? Two observations indicate that the inactivation of HERG channels and that of KvLQT1

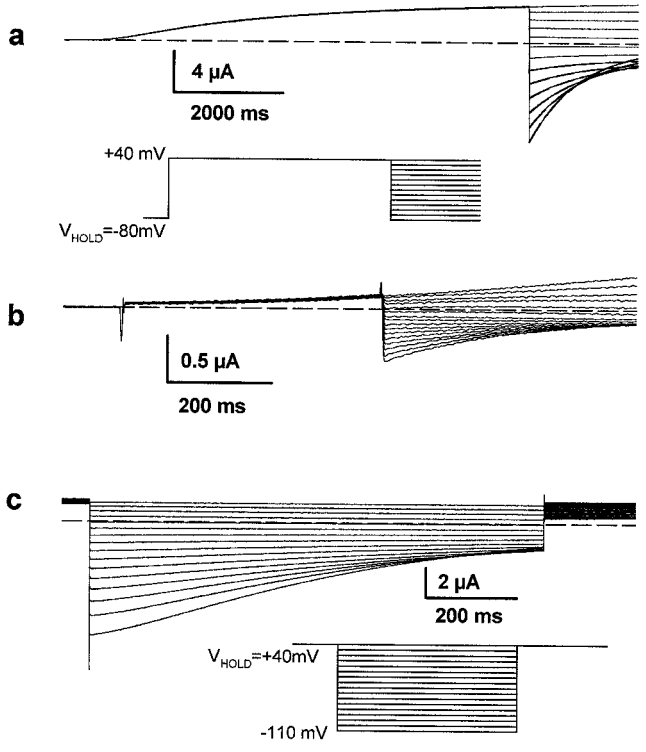

FIGURE 6 Lack of inactivation in heteromeric KvLQT1/minK channels. Tail currents of heteromeric KvLQT1/minK channels from the same oocyte in 100 K are shown on a long time scale (*a*) and a faster time scale (*b*). No "hook" in the tail currents is visible. Dashed lines in *a* represent monoexponential fits. (*c*) Currents from a different oocyte expressing KvLQT1/minK were measured in high potassium (the pulse protocol is represented in the *inset*). Waiting time between individual pulses was 20 s. Note the inflection of the tail currents at negative voltages.

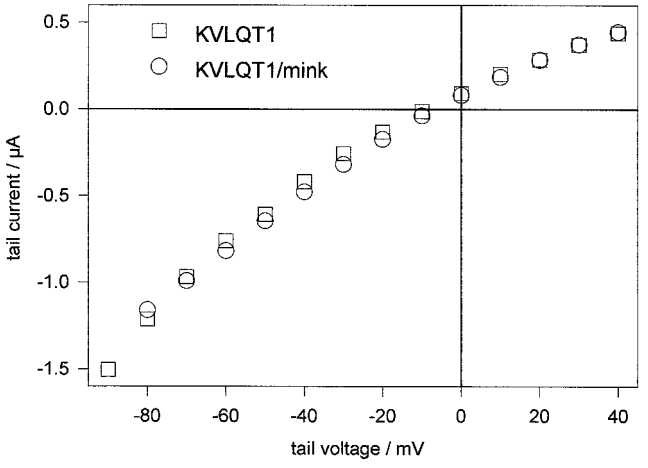

FIGURE 7 Instantaneous current voltage relationship of homomeric KvLQT1 channels and heteromeric KvLQT1/minK channels in high K^+. The instantaneous tail current amplitude was determined from the experiments shown in Figs. 5 *b* and Fig. 6 *a*, respectively, by fitting exponential functions to the tail current and back-extrapolation to the onset of the voltage step. The data for the heteromeric channels were scaled by eye to achieve maximum overlap.

are not equivalent. First, KvLQT1 inactivation is not dependent on extracellular K^+, in contrast to HERG inactivation (Wang et al., 1997) and to classical C-type inactivation (Hoshi et al., 1990; López-Barneo et al., 1993; Baukrowitz and Yellen, 1995). Second, the inactivation of KvLQT1 occurs with a considerable delay after channel activation, whereas HERG inactivation does not show such a delay (Wang et al., 1997). It will be interesting to investigate the possibility that the inactivation process is sensitive to mutations in the pore region, as in the case of HERG (Schönherr and Heinemann, 1996), or to N-terminal deletions, as in the case of N-type inactivation of Shaker K^+ channels (Hoshi et al., 1990). Like the N-type inactivation of Shaker potassium channels, inactivation of KvLQT1 seems to be strongly coupled to activation.

How does the association with the small minK protein result in such large effects on channel gating? It can be speculated that if inactivation occurs, e.g., by plugging the pore from the intracellular side, then minK could interact with the "plug" and prevent it from blocking the heteromeric channel. Identification of the region(s) of the KvLQT1 protein that are involved in the binding of minK will help to answer this question, and it will probably also identify regions that are important for the inactivation process. The fact that mutations in minK can alter the selectivity and the block by cadmium of the K^+ currents obtained after expression of minK in oocytes (Goldstein and Miller, 1991; Tai and Goldstein, 1998; see Kaczmarek and Blumenthal, 1997, for a review) suggests that minK may indeed bind to a part of the KvLQT1 protein that is close to the permeation pathway. A recent study that is consistent with this suggestion showed that the single-channel conductance of homomeric KvLQT1 channels is more than 10-fold larger than that of heteromeric channels (Romey et al., 1997). This finding has recently been challenged, however, by Sesti and Goldstein (1998) and Yang and Sigworth (1998), who report that heteromeric channels have a larger conductance than homomeric ones. Moreover, the ionic selectivity of heteromeric KvLQT1/mink channels seems to be different from that of homomeric KvLQT1 (Wollnik et al., 1997). Yet the form of the instantaneous current-voltage relationship (which reflects the *I-V* of the open channel) in high K^+ is not affected by the association of KvLQT1 with minK (Fig. 7), indicating that not all open-channel properties are changed by minK.

What kind of model can explain the delayed inactivation observed for homomeric KvLQT1? First of all, it is clear that inactivation proceeds at least as fast as activation in the whole range of potentials explored by us (between -40 and $+50$ mV), because otherwise a clear biphasic time course of the current would be observed when the voltage is stepped from a negative holding potential to positive voltages. Furthermore, the recovery from inactivation is faster than channel deactivation, because otherwise the tail currents would have a monotonic time course. A further general consideration is that, although the inactivation process must be voltage dependent to produce the observed effects, the equilibrium distribution between the inactivated state and the most populated open state at large depolarizations must be voltage independent, otherwise all channels would be inactivated at large voltages, in contrast with the observation that steady-state activation and inactivation both approach a plateau above $+40$ mV (see Fig. 4). This consideration excludes sequential gating schemes with only one open state (brackets indicate a set of states):

$$\{C\} \underset{\beta}{\overset{\alpha}{\rightleftarrows}} O \underset{\mu}{\overset{\lambda}{\rightleftarrows}} I$$

Scheme 1

One way to reconcile the apparent voltage dependence of inactivation with an incomplete saturating value of inactivation is to assume that the channels have two open states with different gating charges and that inactivation proceeds only from the open state that is most populated at large positive voltages:

$$\{C\} \underset{\beta}{\overset{\alpha}{\rightleftarrows}} O_1 \underset{\delta}{\overset{\epsilon}{\rightleftarrows}} O_2 \underset{\mu}{\overset{\lambda}{\rightleftarrows}} I$$

Scheme 2

where λ and μ are voltage independent. Scheme 2 predicts that the tail currents relax as a sum of at least three exponentials. A double-exponential decay is obtained if $\alpha = \epsilon = 0$ and δ is much larger than λ. In that case the two time constants are $\tau_s = 1/\beta$ and $\tau_f = 1/\mu$, and the ratio of a_f and a_s would be a fairly good indicator of the probability of being in the inactivated state. Because the experimental values of a_f/a_s are decreasing for $V_t > -100$ mV (Fig. 8 *b*), the consistency with Scheme 2 requires that δ become comparable to or smaller than λ at these potentials. Simulations of Scheme 2 show that also in this case, tail currents can be effectively described by the sum of only two exponentials, because the contributions of the exponentials with the fastest time constants are negligible.

To test if Scheme 2 is indeed compatible with our experimental results, we determined values for the various rate constants and gating charges that gave predictions consistent with the time course of the development of the fast and slow components (a_f, a_s) at various V_p (Fig. 4) and the dependence of tail-current characteristics on V_t. In Fig. 8, *a* and *b*, we plot, respectively, the time constants of the tail currents from Fig. 5 and the ratio a_f/a_s for these tail currents. The solid lines represent the predictions of Scheme 2 with the parameters given in the legend. It can be seen that the model predicts a correct voltage dependence of fast and slow time constants, and a strong dependence of the ratio a_f/a_s on the tail potential. Furthermore, the development of a_f and a_s with t_p at various values of V_p is relatively well fitted (Fig. 4, *dotted lines*). The steady-state values of a_f and a_s estimated from the single-exponential fits in Fig. 4 are

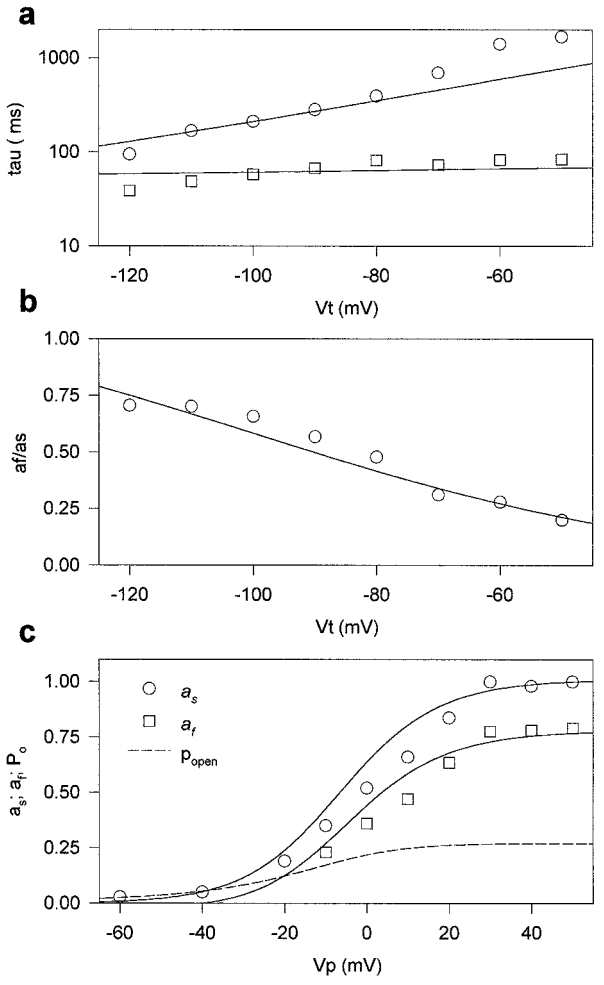

FIGURE 8 Predictions of Scheme 2. In *a* the time constants of the tail currents of Fig. 4 (in high potassium) are replotted, and in *b* the ratio a_f/a_s for these currents is shown. From Scheme 2 we calculated predictions for these quantities, assuming two closed states:

$$C_1 \underset{\beta_1}{\overset{\alpha_1}{\rightleftarrows}} C_2 \underset{\beta_2}{\overset{\alpha_2}{\rightleftarrows}} O_1 \underset{\delta}{\overset{\epsilon}{\rightleftarrows}} O_2 \underset{\mu}{\overset{\lambda}{\rightleftarrows}} I$$

The contribution to tail relaxations from the exponential components with the shortest time constants was negligible. The continuous lines represent the predictions obtained with the parameters (in s^{-1}, $\phi = VF/(RT)$)

$\alpha_1 = 4.6*\exp(0.47\,\phi)$, $\beta_1 = 33*\exp(-0.35\,\phi)$,

$\alpha_2 = 24*\exp(0.006\,\phi)$, $\beta_2 = 19*\exp(-0.007\,\phi)$,

$\epsilon = 4.6*\exp(0.8\,\phi)$, $\delta = 1.4*\exp(-0.7\,\phi)$, $\lambda = 142$, $\mu = 52$

Note that the opening transition C2-O1 is almost voltage-independent. With these values for λ and μ, ~73% of the channels are inactivated at positive voltages. In *c* the extrapolated steady-state values for a_f and a_s obtained from the single exponential fits of Fig. 4 are plotted versus V_p. The continuous lines represent the predictions. The dashed line represents the predicted open probability.

plotted in Fig. 8 *c* (*symbols*) together with the predictions of Scheme 2 (*solid lines*). From these simulations we cannot conclude that the parameters used are the "true" values for the gating of KvLQT1, and we cannot exclude alternative models, especially with more states. The simulations suggest, however, that a gating scheme with two open states and a voltage-independent inactivation process is able to reproduce most of the features of the currents mediated by homomeric KvLQT1 channels.

Interestingly, even though with the estimated values of λ and μ ~73% of the channels are inactivated at the end of a 1-s prepulse to $V_p >= 30$ mV, tail currents at, e.g., $V_t = -60$ mV display only a relatively small "hook." At more negative tail potentials, the ratio a_f/a_s is a better measure of inactivation.

It may be surprising that although 73% of the channels are inactivated at saturating positive voltages ($\geq +30$ mV), the steady-state current-voltage relationship is monotonic (e.g., in Fig. 1 *b* currents increase monotonically with V_p). The dashed line in Fig. 8 *c* shows that the open probability curve predicted by Scheme 2 can indeed have no decline at positive voltages. Moreover, the time course of the open probability after a step to positive voltages from a holding potential of -80 mV is predicted to be monotonic with the appropriate parameters (simulation not shown; parameters are given in the legend to Fig. 8), consistent with the experimental finding. Both of these features arise from having assumed in our model that the C2-O1 transition is weakly voltage-dependent and that the equilibrium voltage of the O1-O_2 transition is much more negative than that of the activating transitions.

We notice that in the limiting case of both λ and μ being much larger than δ, Scheme 2 is equivalent to a scheme with two open states and no inactivation, where the second open state has a lower single-channel conductance. From our measurements we cannot rule out with confidence this possibility. Single-channel recordings showing or not showing the existence of sublevels of the open channel conductance are necessary to provide such information. In summary, we can conclude that Scheme 2 provides a plausible description of our experimental observations, and, more generally, that homomeric KvLQT1 channels probably have at least two open states.

A more solid understanding of the gating and conduction properties of KvLQT1 and minK will also be of significance for an evaluation of the effects of the various mutations of the *KVLQT1* gene in patients with the dominant LQT syndrome (Russell et al., 1996; Wollnik et al., 1997; Tanaka et al., 1997; Van den Berg et al., 1997; Chouabe et al., 1997) and the recessive Jervell-Lange-Nielsen syndrome (Neyroud et al., 1997; Chouabe et al., 1997), and for the recently found mutations in the human *MINK* gene (Splawski et al., 1997; Schulze-Bahr et al., 1997).

If in vivo KvLQT1 is always associated in a heteromeric complex with minK or related proteins, the inactivation process of homomeric KvLQT1 channels may have minor physiological importance. It cannot be excluded, however, that not all KvLQT1 channels are associated with minK, in which case the degree of minK expression could serve as a regulatory mechanism of the properties of the delayed rectifier current.

We thank Enrico Gaggero for construction of the voltage-clamp amplifier.

This work was supported by Telethon-Italy (grant 926).

REFERENCES

Balser, J. R., P. B. Bennett, and D. M. Roden. 1990. Time-dependent outward current in guinea pig ventricular myocytes. *J. Gen. Physiol.* 96:835–863.

Barhanin, J., F. Lesage, E. Guillemare, M. Fink, M. Lazdunski, and G. Romey. 1996. K(V)LQT1 and lsK (minK) proteins associate to form the *I*(Ks) cardiac potassium current. *Nature.* 384:78–80.

Baukrowitz, T., and G. Yellen. 1995. Modulation of K^+ current by frequency and external $[K^+]$: a tale of two inactivation mechanisms. *Neuron.* 15:951–960.

Caceci, M. S., and W. P. Cacheris. 1984. Fitting curves to data. The simplex algorithm is the answer. *Byte.* 9:340–362.

Campbell, D. L., R. L. Rasmusson, and H, C. Strauss. 1992. Ionic current mechanisms generating vertebrate primary pacemaker activity at the single cell level: an integrative view. *Annu. Rev. Physiol.* 54:279–302.

Chouabe, C., N. Neyroud, P. Guicheney, M. Lazdunski, G. Romey, and J. Barhanin. 1997. Properties of KvLQT1 K^+ channel mutations in Romano-Ward and Jervell and Lange-Nielsen inherited cardiac arrhythmias. *EMBO J.* 16:5471–5479.

Curran, M. E., I. Splawski, K. W. Timothy, G. M. Vincent, E. D. Green, and M. T. Keating. 1995. A molecular basis for cardiac arrhythmia: HERG mutations cause long QT syndrome. *Cell.* 80:795–803.

DiFrancesco, D. 1985. The cardiac hyperpolarizing-activated current, I_f. Origins and developments. *Prog. Biophys. Mol. Biol.* 46:163–183.

Goldstein, S. A. N., and C. Miller. 1991. Site-specific mutations in a minimal voltage-dependent K^+ channel alter ion selectivity and open-channel block. *Neuron.* 7:403–408.

Hoshi, T., W. N. Zagotta, and R. W. Aldrich. 1990. Biophysical and molecular mechanisms of Shaker potassium channel inactivation. *Science.* 250:533–538.

Jurkiewicz, N. K., and M. C. Sanguinetti. 1993. Rate dependent prolongation of cardiac action potentials by a methanesulfamilide agent. Specific block of rapidly activating delayed rectifier K^+ current by dofetilide. *Circ. Res.* 72:75–83.

Kaczmarek, L. K., and E. M. Blumenthal. 1997. Properties and regulation of the minK potassium channel protein. *Physiol. Rev.* 77:627–641.

López-Barneo, L., T. Hoshi, S. H. Heinemann, and R. W. Aldrich. 1993. Effects of external cations and mutations in the pore region on C-type inactivation of Shaker potassium channels. *Receptors Channels.* 1:61–71.

McDonald, T. V., Z. Yu, Z. Ming, E. Palma, M. B. Meyers, K.-W. Wang, S. A. N. Goldstein, and G. I. Fishman. 1997. A minK-HERG complex regulates potassium current I_{Kr}. *Nature.* 388:289–292.

Neyroud, N., F. Tesson, I. Denjoy, M. Leibovici, C. Donger, J. Barhanin, S. Fauré, F. Gary, P. Coumel, C. Petit, K. Schwartz, and P. Guicheney. 1997. A novel mutation in the potassium channel gene KvLQT1 causes the Jervell and Lange-Nielsen cardioauditory syndrome. *Nature Genet.* 15:186–189.

Noble, D. 1984. The surprising heart: a review of recent progress in cardiac electrophysiology. *J. Physiol. (Lond.).* 353:1–50.

Roden, D. M., and A. L. George, Jr. 1996. The cardiac ion channels: relevance to management of arrhythmias. *Annu. Rev. Med.* 47:135–148.

Romey, G., B. Attali, C. Chouabe, I. Abitbol, E. Guillemare, J. Barhanin, and M. Lazdunski. 1997. Molecular mechanism and functional significance of the MinK control of the KvLQT1 channel activity. *J. Biol. Chem.* 272:16713–16716.

Russell, M. W., M. Dick, II, F. S. Collins, and L. C. Brody. 1996. KvLQT1 mutations in three families with familial or sporadic long QT syndrome. *Hum. Mol. Genet.* 5:1319–1324.

Sanguinetti, M. C., M. E. Curran, A. Zou, J. Shen, P. S. Spector, D. L. Atkinson, and M. T. Keating. 1996. Coassembly of K(V)LQT1 and minK (IsK) proteins to form cardiac *I*(Ks) potassium channel. *Nature.* 384:80–83.

Sanguinetti, M. C., C. Jiang, M. E. Curran, and M. T. Keating. 1995. A mechanistic link between an inherited and an acquired cardiac arrhythmia: HERG encodes the I_{Kr} potassium channel. *Cell.* 81: 299–307.

Schönherr, R., and Heinemann, S. H. 1996. Molecular determinants for activation and inactivation of HERG, a human inward rectifier potassium channel. *J. Physiol. (Lond.).* 493:635–642.

Schulze-Bahr, E., Q. Wang, H. Wedekind, W. Haverkamp, Q. Chen, Y. Sun, C. Rubie, M. Hördt, J. A. Towbin, M. Borggrefe, G. Assmann, X. Qu, J. C. Somberg, G. Breithardt, C. Oberti, and H. Funke. 1997. KCNE1 mutations cause Jervell and Lange-Nielsen syndrome. *Nature Genet.* 17:267–268.

Sesti, F., and A. N. Goldstein. 1998. IKs channels: minK/KvLQT1 heteromultimers have a larger unitary conductance than homomeric KvLQT1 channels. *Biophys. J.* 74:A346 (Abstr.).

Smith, P. L., T. Baukrowitz, and G. Yellen. 1996. The inward rectification mechanism of the HERG cardiac potassium channel. *Nature.* 379: 833–836.

Spector, P. M., M. E. Curran, A. R. Zou, and M. C. Sanguinetti. 1996. Fast inactivation causes rectification of the IKr channel. *J. Gen. Physiol.* 107:611–619.

Splawski, I., M. Tristani-Firouzi, M. H. Lehmann, M. C. Sanguinetti, and M. T. Keating. 1997. Mutations in the hminK gene cause long QT syndrome and suppress IKs function. *Nature Genet.* 17:338–340.

Tai, K.-K., and S. A. N. Goldstein. 1998. The conduction pore of a cardiac potassium channel. *Nature.* 391:605–608.

Takumi, T., H. Ohkubo, and S. Nakanishi. 1988. Cloning of a membrane protein that induces a slow voltage-gated potassium current. *Science.* 242:1042–1045.

Tanaka, T., R. Nagai, H. Tomoike, S. Takata, K. Yano, K. Yabuta, N. Haneda, O. Nakano, A. Shibata, T. Sawayama, H. Kasai, Y. Yazaki, and Y. Nakamura. 1997. Four novel KvLQT1 and four novel HERG mutations in familial long-QT syndrome. *Circulation.* 95:565–567.

Tristani-Firouzi, M., P. S. Spector, A. Zou, M. T. Keating, and M. C. Sanguinetti. 1997. Voltage-dependent kinetics of KvLQT1, a novel delayed rectifier K^+ channel. *Biophys. J.* 72:A139 (Abstr.).

Trudeau, M. C., J. W. Warmke, B. Ganetzky, and G. A. Robertson. 1995. HERG, a human inward rectifier in the voltage-gated potassium channel family. *Science.* 269:92–95.

Van den Berg, M. H., A. A. M. Wilde, E. O. Robles de Medina, H. Meyer, J. L. M. C. Geelen, R. J. E. Jongbloed, H. J. J. Wellens, and J. P. M. Geraedts. 1997. The long QT syndrome: a novel missense mutation in the S6 region of the KvLQT1 gene. *Hum. Genet.* 100:356–351.

Wang, Q., M. E. Curran, I. Splawski, T. C. Burn, J. M. Millholland, T. J. VanRaay, J. Shen, K. W. Timothy, G. M. Vincent, T. de Jager, P. J. Schwartz, J. A. Toubin, A. J. Moss, D. L. Atkinson, G. M. Landes, T. D. Connors, and M. T. Keating. 1996a. Positional cloning of a novel potassium channel gene: KvLQT1 mutations cause cardiac arrhythmias. *Nature Genet.* 12:17–23.

Wang, S., S. Liu, M. J. Morales, H. C. Strauss, and R. L. Rasmusson. 1997. A quantitative analysis of the activation and inactivation kinetics of HERG expressed in *Xenopus* oocytes. *J. Physiol. (Lond.).* 502:45–60.

Wang, S., M. J. Morales, S. Liu, H. C. Strauss, and R. L. Rasmusson. 1996b. Time-, voltage- and ionic-concentration dependence of rectification of h-erg expressed in *Xenopus* oocytes. *FEBS Lett.* 38:167–173.

Wollnik, B., B. C. Schroeder, C. Kubisch, H. D. Esperer, P. Wieacker, and T. J. Jentsch. 1997. Pathophysiological mechanisms of dominant and recessive KvLQT1 K^+ channel mutations found in inherited cardiac arrhythmias. *Hum. Mol. Genet.* 6:1943–1949.

Yang, W. P., P. C. Levesque, W. A. Little, M. L. Conder, F. Y. Shalaby, and M. A. Blanar. 1997. KvLQT1, a voltage-gated potassium channel responsible for human cardiac arrhythmias. *Proc. Natl. Acad. Sci. USA.* 94:4017–4021.

Yang, Y., and F. J. Sigworth. 1998. The conductance of KvLQT1 channels. *Biophys. J.* 74:A19 (Abstr.).